Support information for RSC advances

Enhance luminescence and tuning magnetic properties of lanthanide coordination polymers based on fluorine substituted and phenanthroline ligands

Xun Feng*[a], Yapei Shang[c, a], Heng Zhang[c, a], Rongfang Li[a], Weizhou Wang[a], Daoming Zhang[a], Liya Wang*[a ,b ‡], Zhongjun Li[c]

[a]College of Chemistry and Chemical Engineering and Henan Key Laboratory of Function Oriented Porous Materials, Luoyang Normal University, Luoyang, 471934, China

[b] College of Chemistry and Pharmacy Engineering, Nanyang Normal University, Nanyang, 473601, China

[c] College of Chemistry and Molecular Engineering, Zhengzhou University, Zhengzhou, 450001, China

Table of Contents

1 Experimental Section

1.1 Materials and Instrumentation

All reagents used in the syntheses were of analytical grade, and used without further purification. Elemental analyses for carbon, hydrogen and nitrogen atoms were performed on a Vario EL III elemental analyzer. The infrared spectra (4000 ~ 500 cm^{-1}) were recorded by using KBr pellet on an AvatarTM 360 E. S. P. IR spectrometer. The crystal determination was performed on a Bruker SMART APEX II CCD diffractometer equipped with graphite-monochromatized Mo$K\alpha$ radiation (λ = 0.71073 Å). Thermo gravimetry differential thermal analysis was recorded using a SDT 2960 simultaneous thermal analyzer (DTA Instruments, New Castle, DE) in N_2 atmosphere at a heating rate of 10 °C min^{-1} from 20 to 1000 °C. Variable-temperature magnetic susceptibilities were measured using a MPMS-7 SQUID magnetometer under a 0.1 T applied magnetic field and over the range of 1.8 to 300 K. The experimental susceptibilities were corrected for the diamagnetism of the constituent atoms using Pascal' s tables. The visible phosphorescence spectrum was recorded on a Hitachi F-7000 fluorescence spectrophotometer. The NIR luminescence properties were recorded using an FLS 1000 Edinburgh Analytical Instrument furnished by a 450 W xenon lamp and a μF900H high-energy microsecond flash lamp as the excitation sources. The emission quantum yields were measured at room temperature using a Quantum Yield Measurement System (Hamamatsu C11347-12 QY spectrometer) with a 450W Xe lamp coupled to a monochromator for wavelength discrimination, an integrating sphere as sample chamber. The powder X-ray diffraction (PXRD) patterns were measured using a Bruker D8 Advance powder diffractometer at 40 kV, 40 mA for Cu Kα radiation (λ = 1.5418 Å), with a scan speed of 0.2 s/step and a step size of 0.02 (2θ) in the range of 2θ = 5−50°.

1.2 Synthesis of series coordination polymers 2-7

The same procedure for polymer **1** was employed in preparation polymers **2-7**.

H_2Tfpda acid (0.0483g, 0.2 mmol) and phen (0.0381 g, 0.22 mmol) in a solution of water / alcohol (v/v =1.5, 10 mL) were mixed with an aqueous solution (10 mL) of lanthanide(III) nitrate hexahydrate (**2**) = $Nd(NO_3)_3\cdot 6H_2O$, 0.080 g,0.2 mmol, pH=3.0; (**3**)= $Dy(NO_3)_3\cdot 5H_2O$, 0.081 g; (**4**)= $Ho(NO_3)_3\cdot 5H_2O$, 0.082 g; (**5**) = $Er(NO_3)_3\cdot 6H_2O$, 0.083 g; (**6**)= $Yb(NO_3)_3\cdot 6H_2O$ 0.082 g; (**7**)= $Gd(NO_3)_3\cdot 6H_2O$, 0.083 g) were mixed in an ethanol-water solution. After stirring for 30 min in air, the aqueous mixture was placed into 25 mL Teflon-lined autoclave under autogenous pressure being heated at 140 °C for 72 h, and then the autoclave was cooled over a period of 24 h at a rate 5 °C/h. Light red blocks crystals of (**2**) were obtained suitable for X-ray diffraction analysis. For (**2**), yield: 0.0395 g (50%). Elemental analysis (%): calcd for $C_{40}H_{19}F_8N_4NdO_9$: C 48.24, H 1.94, N 5.63, found: C 48.26, H 1. 92, N 5.60. IR: 3346s, 2818m, 1618s, 1446vs, 1379m, 1078m, 824m, 729(m), 667(m). For (**3**), yield: 0.0341 g (43%). Elemental analysis (%): calcd for $C_{75}H_{31}Dy_3F_{20}N_6O_{21}$: C 40.58, H 1.42, N 3.76, found: C 40.09, H 1. 43, N 3.74. IR: 3325s, 3006br, 1656s, 1563sh, 1475vs, 1127m, 1009s, 856m, 687m. For (**4**), yield: 0.0298 g (38%). Elemental analysis (%): calcd for $C_{48}H_{24}F_{12}Ho_2N_4O_{16}$, C 39.29, H 1.65, N 3.81, found: C 40.02, H 1.63, N 3. 91. IR: 3432s, 2947m, 1603s, 1462s, 1374s, 1017m, 829s. For (**5**), yield: 0.0298 g (38%).

Elemental analysis (%): calcd for $C_{75}H_{31}Er_3F_{20}N_6O_{21}$, C 40.33, H 1.39, N 3.76, found: C 40.22, H 1.31, N 3.179. IR: 3362s, 3007br, 1603s, 1374s, 1017s, 856m, 687s. For (**6**), yield: 0.0341 g (43%). Elemental analysis (%): calcd for $C_{75}H_{31}F_{20}N_6O_{21}Yb_3$: C 40. 01, H 1.39, N 3.73, found: C 39.87, H 1.29, N 3.74. IR: 3215br, 1613s, 1572vs, 1012s, 832s. For (**7**), yield: 44%. Anal (%). Calc.: for $C_{48}H_{24}F_{12}N_4O_{16}Gd_2$. C, 39.62; N, 3.85; H, 1.67. Found: C, 39.70; N, 3.83; H, 1.72%. Selected IR (KBr pellet, cm-1): 3365(vs), 1642(vs), 1520(s), 1432(vs), 1400(s), 1263(s), 1143(m), 1070(s), 943(m), 865(m), 8774(m), 723(m), 657(s).

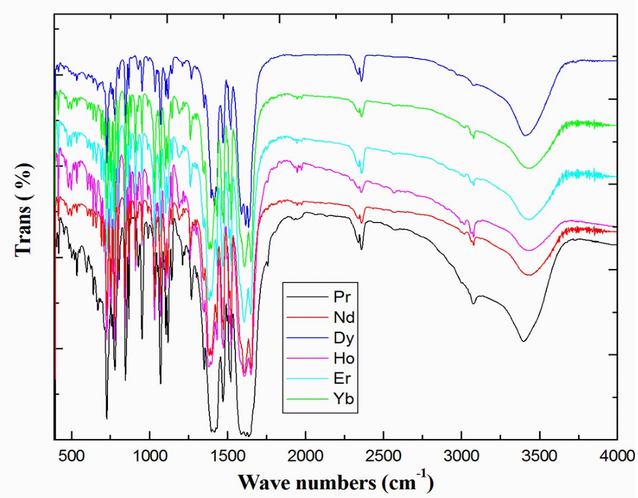

Figure S1. Fourier transforms infrared spectra of coordination polymers **1**- **6**.

2. IR spectra

In the IR spectra of **1** - **6** (see Figure Sure S1, supporting information), the board strong absorption peaks in the frequency region of 3300-3500 cm^{-1} are attributed to O-H unsaturated stretching vibration of water molecules. The weak peaks at 3000 cm^{-1} correspond to asymmetric stretching vibrations for C-H from phen. The sharp bands in the ranges of 1600-1530 and 1450-1380 cm^{-1} are attributed to asymmetric and symmetric stretching vibrations of carboxylic groups, respectively [1]. The strong peaks about 1300-1100 cm^{-1} are attributed to C-F stretching vibration of substituted benzene ring. The peaks about 596 cm^{-1} are attributed to bending vibration C-F group attached to the benzene ring [2]. The IR spectra indicate the presence both bridging and bidentate chelating coordination modes in series of compounds, by calculating the frequency separation between asymmetric and symmetric stretching frequency of carboxylic group based on Deacon–Philips rule [3].

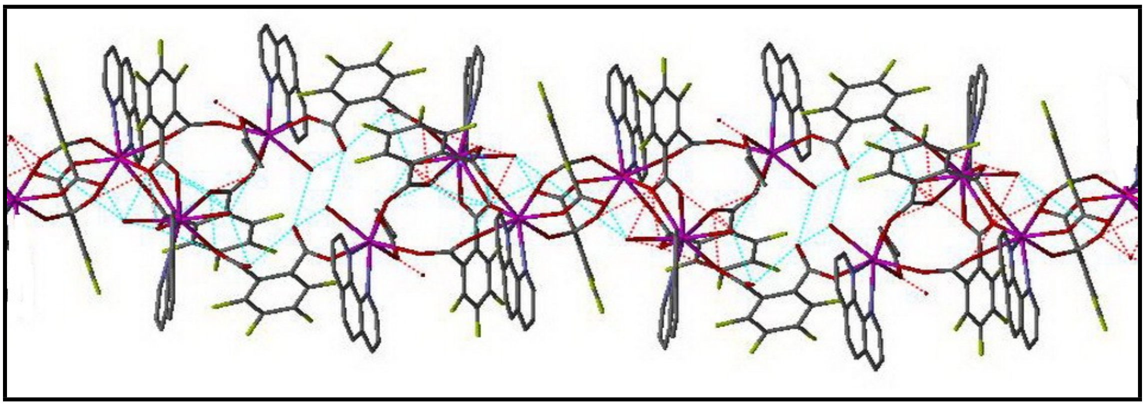

Figure S2. Diamond illustration of Tfpa propagating the binuclear [Pr_2Tfpaphen] units into 1D alternate chain assisted through the intermolecular hydrogen bonding in **1**.

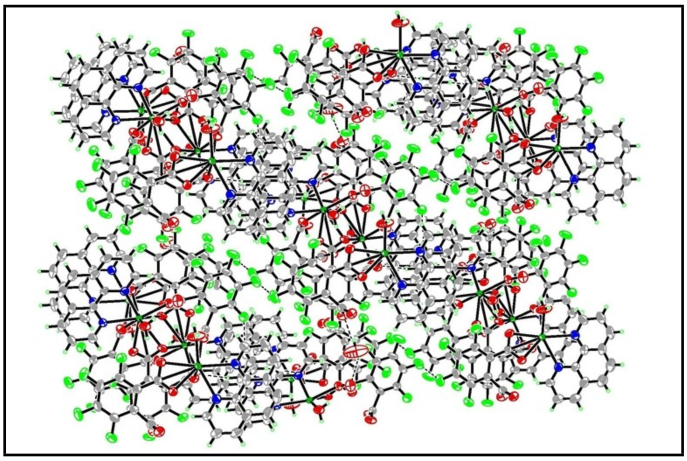

Figure S3. Projection view of the 3D pack arrangement in polymer **1** along *ab* plane.

3. Crystal Structure analysis of 2

Single-crystal X-ray diffraction study reveals that complex **2** crystallize in the triclinic system, space group of P_{-1}. The asymmetric unit of the complex is composed of one independent Nd(III) ion, four H_2Tfpa ligands, two phen ligands, one coordinating water molecule and one uncoordinated Phen moiety. The central ion is a nine-coordinated, with a N_2O_7 donor set, among which six O atoms are derived from the H_2Tfpa ligand (O1; O1#1; O2#1; O3; O5; O6#1), an oxygen is from the coordinating water molecule, and two N atoms (N1; N2) from the Phen ligand complete a distorted mono-capped tetragonal prism geometry. Furthermore, the Tfpa^{2-}ligands with complete deprotonation form, Tfpa^{2-} connected to two adjacent Nd (III) ions *via* two modes: bridging (μ2-η1: η1) and chelating (μ2-η2: η1). The high pH leaving one protonated carboxylic group in H_2Tfpa ligand, which is essentially different from the other coordination polymers in this series, where the distance between the centers of the two Nd(III) ions is 4.0542(1) Å. The bond length of Nd(III)-O of the polymer is 2.4280(17) Å to

2.7097(18) Å, and the average bond length of Nd(III)-O(1W) is 2.465 Å. The average bond length Nd(III)-N is found to be 2.617(2) Å . (μ2 -Tfpa^{2-} ligand bridged the asymmetric units into binuclear cluster in a face-to-face orientation. The strong hydrogen bonding between F atoms of Tfpa ligands and O atoms from water were observed, the binuclear clusters are further linked together by Nd(III) ion, generating a discrete zero -dimensional (0D) binuclear rectangular structure, leaving free Phen moieties on two sides.

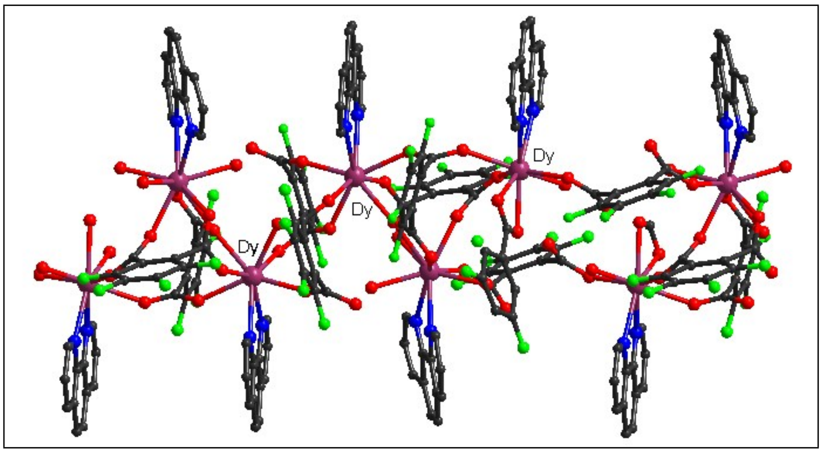

Figure S4. 1D chain structure constructed from the trinuclear clusters SBU.

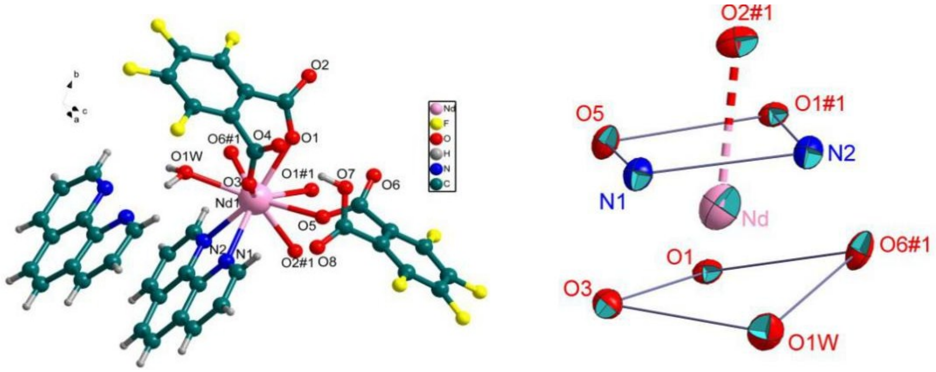

(a) (b)

Figure S5. (a) Asymmetric coordination unit of **2**. (b) Coordination model of central ion in **2**.

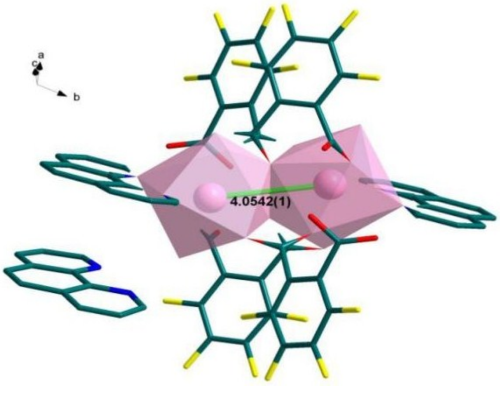

Figure S6. Diamond illustration of binuclear unit in **2.**

4 Additional Figures

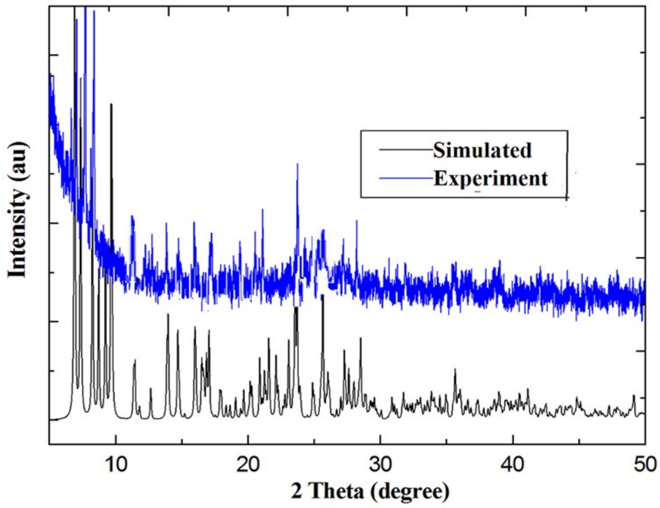

Figure S7. Comparison of stimulated (blue) and experimental (red) powder XRD patterns of coordination polymer Nd (**2**).

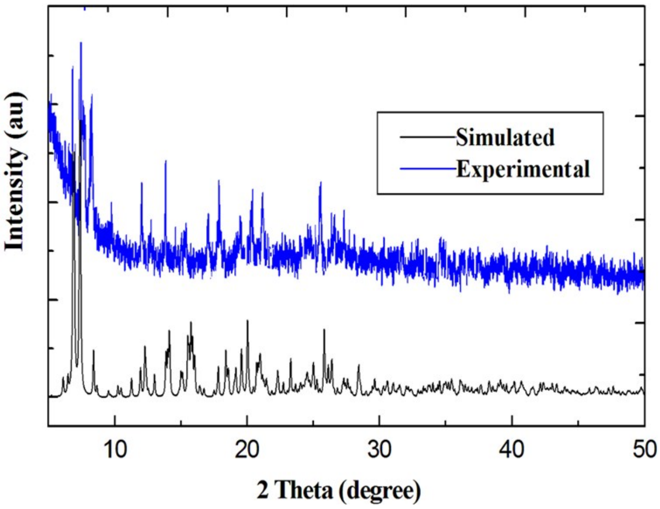

Figure S8. Comparison of stimulated (blue) and experimental (red) powder XRD patterns of Dy coordination polymer (**3**).

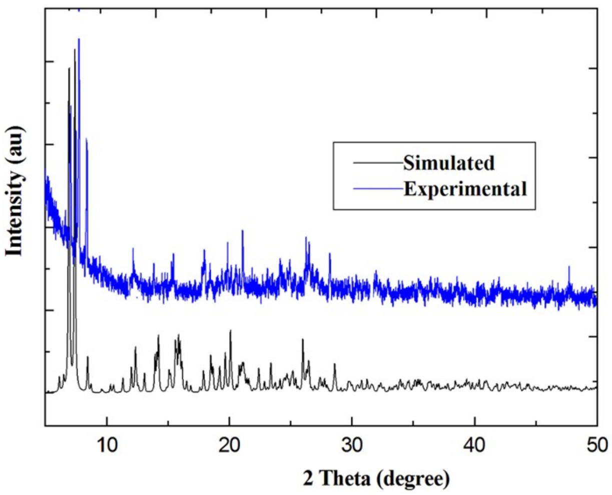

Figure S9. Comparison of stimulated (blue) and experimental (red) powder XRD patterns of Ho coordination polymer (**4**) .

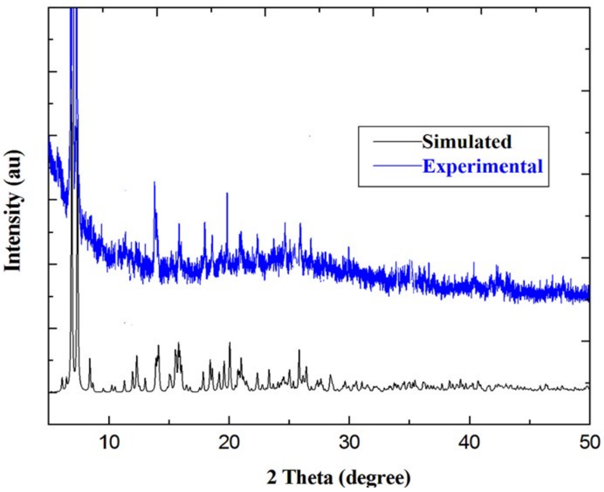

Figure S10. Comparison of stimulated (blue) and experimental (red) powder XRD patterns of Er coordination polymer **5**.

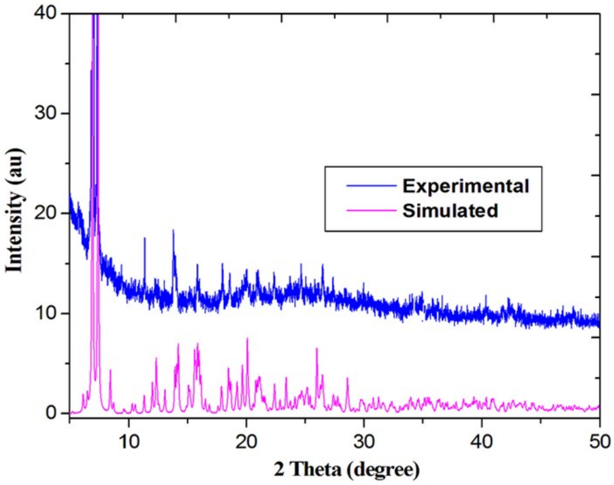

Figure S11. Comparison of stimulated (blue) and experimental (pink) PXRD patterns of **6** (**Yb**).

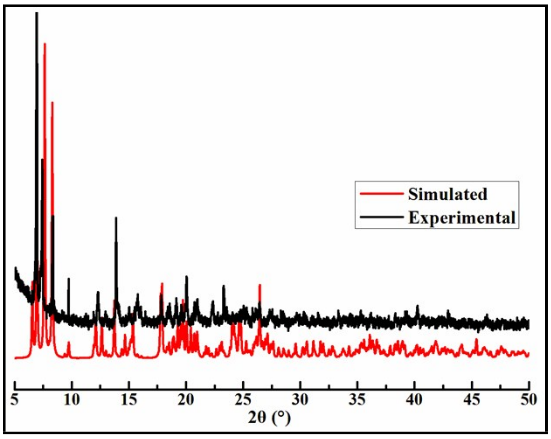

Figure S12. Comparison of stimulated (red) and experimental (black) PXRD patterns of **7**(**Gd)**.

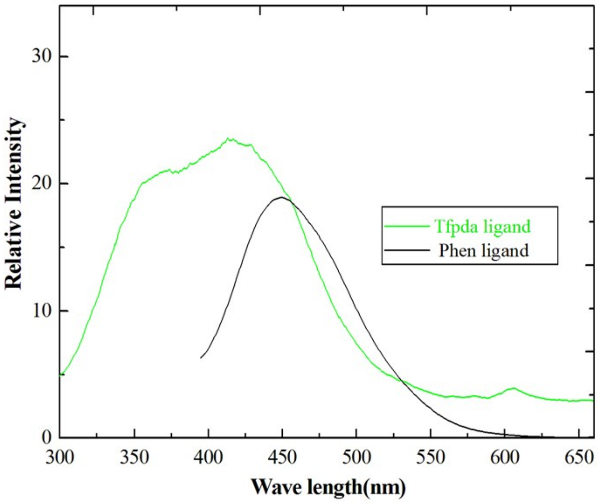

Figure S13. Emission spectra of free Phen and H_2Tfpda ligands (excited at 297 nm)

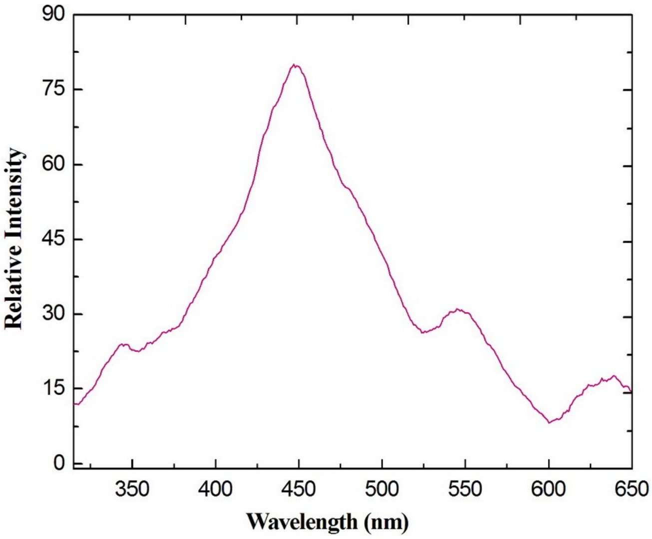

Figure S14.The phosphorescence spectrum of Gd(III) compound **7** (77 K, excited at 297 nm).

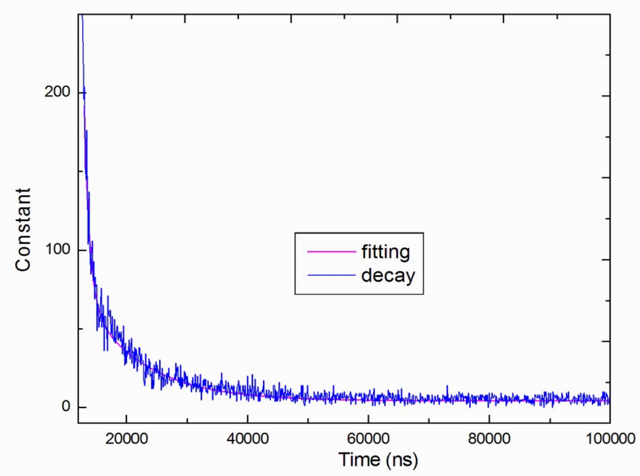

Figure S15. Phosphorescence decay curves of Pr(III) coordination polymer (**1**).

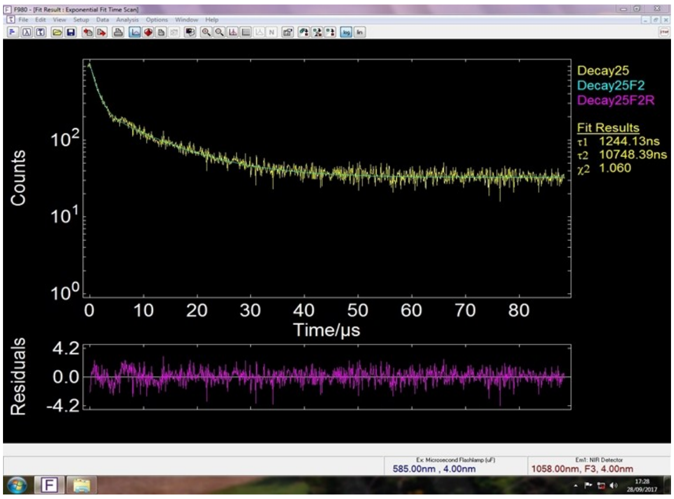

Fit Results
τ1 1244.13ns
τ2 10748.39ns
χ2 1.060

Ex: Microsecond Flashlamp (uF)
585.00nm , 4.00nm

Em1: NIR Detector
1058.00nm, F3, 4.00nm

17:28
28/09/2017

Figure S16. Phosphorescence decay curves of Nd(III) coordination polymer (**2**).

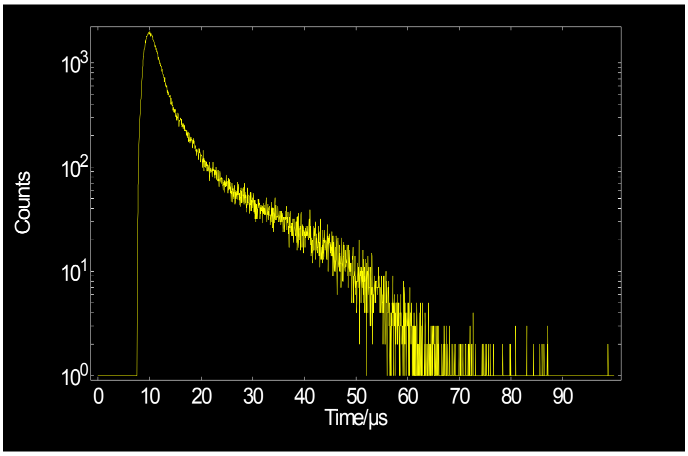

Figure S17. Phosphorescence decay curves of Dy(III) coordination polymer (**3**).

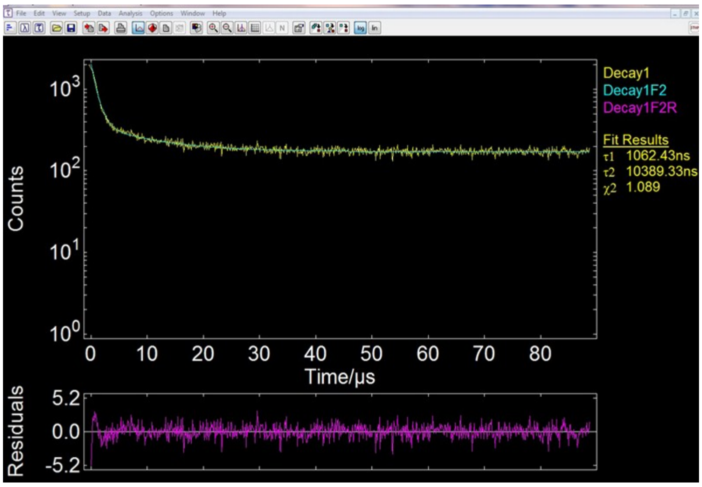

Fit Results
τ1 1062.43ns
τ2 10389.33ns
χ2 1.089

Figure S18. Phosphorescence decay curves of Ho(III) coordination polymer (**4**).

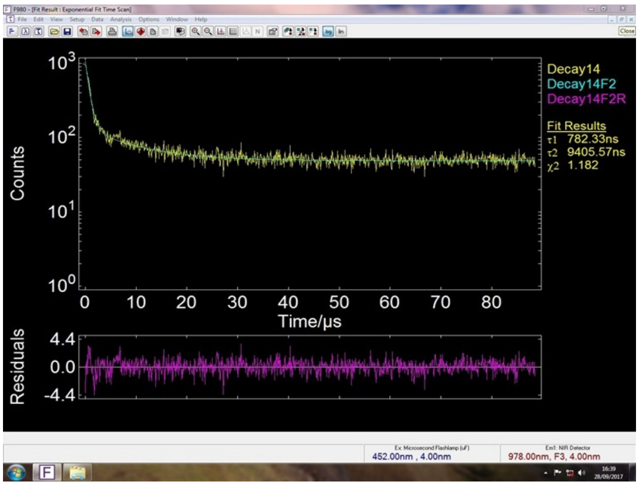

Fit Results
τ1 782.33ns
τ2 9405.57ns
χ2 1.182

Ex: Microsecond Flashlamp (uF) 452.00nm , 4.00nm

Em1: NIR Detector 978.00nm, F3, 4.00nm

Figure S19. Phosphorescence decay curves of Er(III) coordination polymer (**5**)

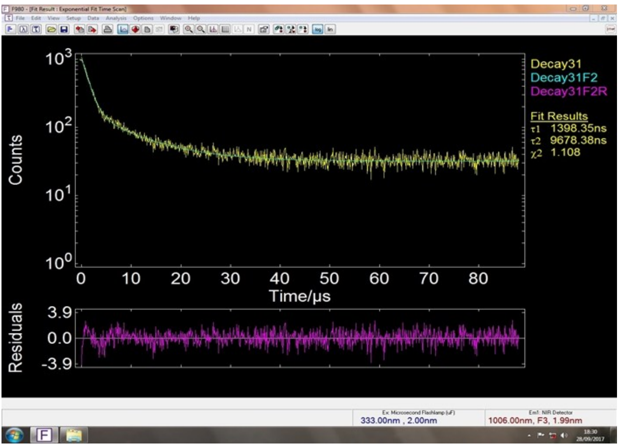

Fit Results
τ1 1398.35ns
τ2 9678.38ns
χ2 1.108

Ex: Microsecond Flashlamp (uF) 333.00nm , 2.00nm

Em1: NIR Detector 1006.00nm, F3, 1.99nm

Figure S20.Phosphorescence decay curves of Yb(III) coordination polymer **6**.

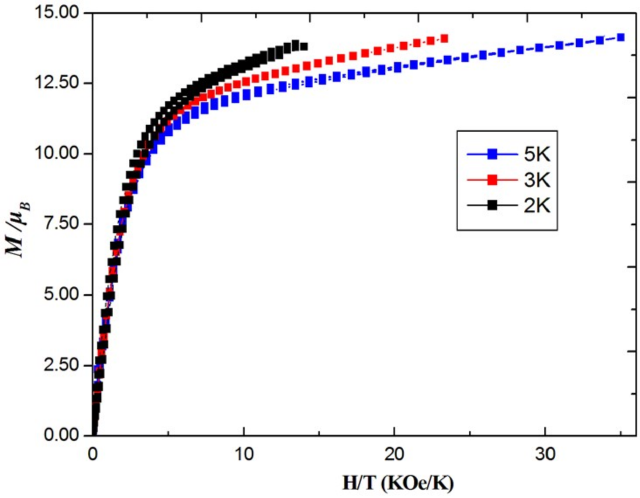

Figure S21. Magnetization vs H/T plots at different temperatures below 70 kOe for **3**.

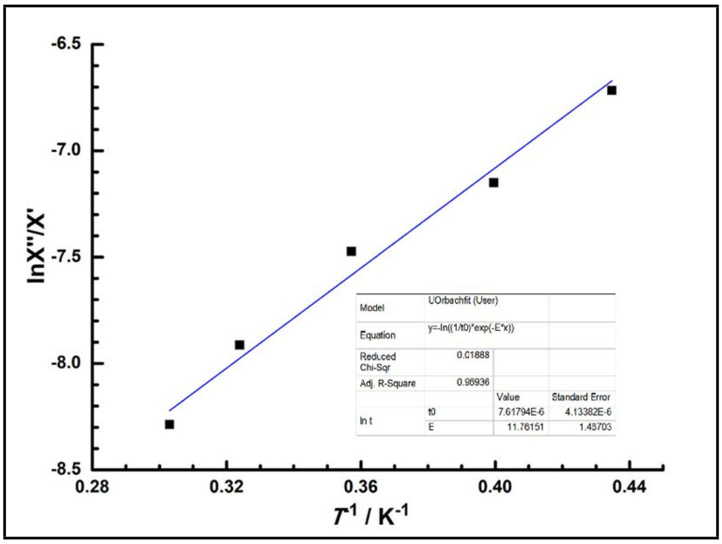

Model	UOrbachfit (User)		
Equation	y=-ln((1/t0)*exp(-E*x))		
Reduced Chi-Sqr	0.01888		
Adj. R-Square	0.96936		
		Value	Standard Error
ln t	t0	7.61794E-6	4.13382E-6
	E	11.76151	1.48703

Figure S22. Temperature dependence of the relaxation time (τ) under a 500 Oe d.c. field. The solid red line is the best fit to the Arrhenius law.

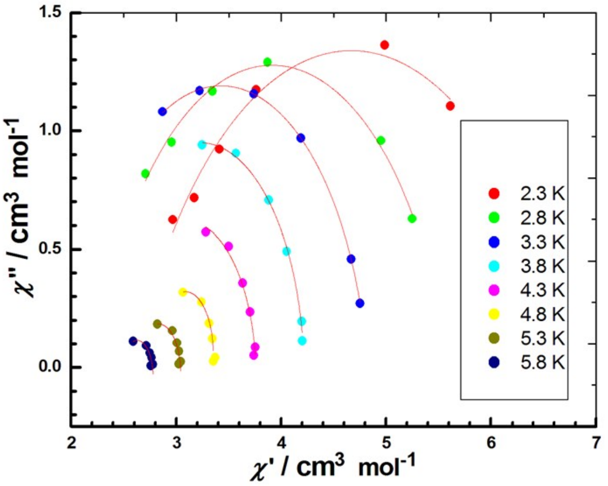

Figure S23. Cole-Cole plots under a 500 Oe d.c. field. The solid lines represent a best fit to the generalized Debye model.

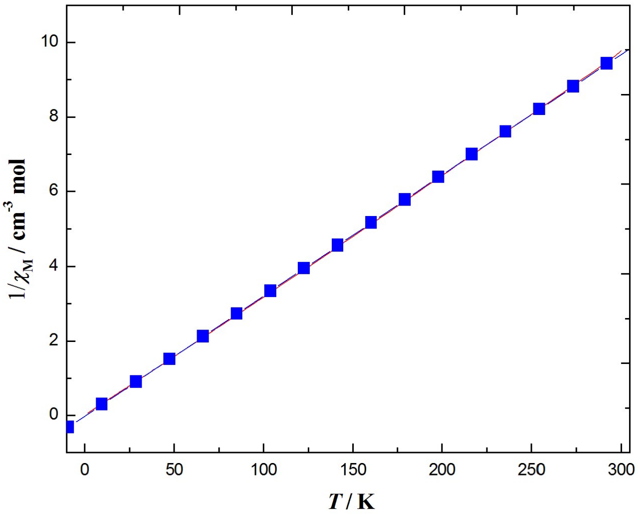

Figure S24. Plots of temperature dependence of reciprocal χ_M for compound **7** (Gd).

The deep red solid lines represent the best fit to the data.

5 . Additional Tables

Table S1. Crystal data and structure refinements for coordination polymer **7**

Compounds No .	**7 Gd**
Empirical formula	$C_{48}H_{24}F_{12}Gd_2N_4O_{16}$
Formula weight	1455.21
Temperature(K)	293(2)
Crystal system	Triclinic
Space group	P_{-1}
a(Å)	13.9646(6)
b(Å)	14.1651(5)
c(Å)	15.0370(6)
α (°)	63.655(4)
β (°)	81.083(3)
γ (°)	65.489(4)
Volume(Å^3)	2423.8(2)
Z	2
D_{caled}(g/cm^3)	1.994
M(mm^{-1})	2.837
F(000)	1408.0
Crystal size(Å$^)$	0.20 × 0.10× 0.05
Radiation	MoKα
2Θ range for data collection(°)	6.438- 53.816
Index ranges	$-17 \leq h \leq 17$ $-17 \leq k \leq 17$ $-18 \leq l \leq 18$
Reflections collected	30103
Independent reflections	8683 [R_{int} = 0.0318
Data/restraints/parameters	8683/17/760
Goodness-of-fit on F^2	0.997
Final R indexes [I>=2σ (I)]	R_1 = 0.0266, wR_2 = 0.0589
Final R indexes [all data]	R_1 = 0.0334 wR_2 = 0.0621
Largest diff. peak/hole / e Å^{-3}	0.68/-0.77

$R = \sum||F_0|-|F_c||/\sum|F_0|$, $_{w}R=\{\sum[_{w}(F_0^2- F_c^2)^2]/ \sum(F_0^2)^2\}^{1/2}$

Table S2. Selected bond lengths [Å] for coordination polymers **1-6**

Compound 1					
Bond	Å	Bond	Å	Bond	Å
Pr(1)-O(1)	2.356(2)	Pr(1)-O(3)	2.578(2)	Pr(2)-O(11^{2})	2.265(2)
Pr(1)-O(5)	2.356(2)	Pr(1)-N(1)	2.579(3)	Pr(2)-O(2)	2.296(2)
Pr(1)-O(8^{1})	2.378(3)	O(11)-Pr(2^{2})	2.265(2)	Pr(2)-O(7^{1})	2.388(2)
Pr(1)-O(4^{1})	2.415(3)	Pr(1)-N(2)	2.611(3)	Pr(2)-O(2W)	2.413(3)
Pr(1)-O(1W)	2.426(3)	Pr(1)-O(3^{1})	2.738(2)	Pr(2)-O(10)	2.417(2)
Pr(2)-O(9)	2.479(3)	Pr(2)-N(4)	2.586(3)	O(4)-Pr(1^{1})	2.415(3)
Pr(2)-N(3)	2.530(3)	O(3)-Pr(1^{1})	2.738(2)	O(7)-Pr(2^{1})	2.388(2)
Compound 2					
Bond	Å	Bond	Å	Bond	Å
Nd(1)-Nd(01^{1})	4.0539(3)	Nd(1)-O(5)	2.4736(17)	Nd(1)-O(5)	2.4736(17)
Nd(1)-O(1)	2.4276(18)	Nd(1)-O(6^{1})	2.4867(18)	O(4)-Nd(01^{1})	2.7093(18)
Nd(1)-O(3^{1})	2.5360(16)	Nd(1)-O(9)	2.4674(18)	O(3)-Nd(01^{1})	2.5359(16)
Nd(1)-O(3)	2.4388(17)	Nd(1)-N(1)	2.600(2)	O(6)-Nd(01^{1})	2.4866(18)
Nd(1)-O(4^{1})	2.7093(19)	Nd(1)-N(2)	2.635(2)	Nd(1)-Nd(01^{1})	4.0539(3)
Compound 3					
Bond	Å	Bond	Å	Bond	Å
Dy(1)-O(1)	2.317(4)	O(10)-Dy(1^{1})	2.427(4)	Dy(3)-O(15)	2.409(4)
Dy(1)-N(2)	2.558(6)	O(12)-Dy(1^{1})	2.369(4)	Dy(3)-O(16)	2.340(4)
Dy(2)-O(5)	2.430(3)	O(16)-Dy(3^{2})	2.340(4)	Dy(3)-N(5)	2.559(5)
Dy(2)-O(6)	2.406(3)	Dy(1)-O(1)	2.317(4)	Dy(3)-N(6)	2.558(5)
Dy(2)-O(11)	2.310(5)	Dy(2)-N(4)	2.530(5)	Dy(2)-O(21)	2.421(4)
Dy(2)-O(4)	2.292(5)	Dy(3)-O(8)	2.364(5)	Dy(2)-N(3)	2.508(6)
Dy(2)-O(7)	2.321(4)	Dy(3)-O(9)	2.379(4)	Dy(3)-O(14)	2.327(4)
Compound 4					
Bond	Å	Bond	Å	Bond	Å
Ho(1)-O(1)	2.375(3)	Ho(1)-O(5)	2.381(3)	Ho(1)-O(8)^{1}	2.405(3)
Ho(1)-N(1)	2.610(4)	Ho(1)-N(2)	2.640(3)	Ho(1)-O(3)	2.602(3)
Ho(2)-O(4)#2	2.446(3)	Ho(2)-O(2)	2.321(3)	Ho(2)-N(3)	2.562(4)
Ho(2)-O(10)	2.440(3)	Ho(2)-O(2w)	2.447(4)	Ho(2)-O(9)	2.503(4
Ho(2)-N(3)	2.562(4)	Ho(2)-N(4)	2.617(4)	O(3)-Ho(1) ^{1}	2.720(3)
O(4)-Ho(3)#1	2.720(3)	O(7)-Ho(2)#1	2.412(3)	O(8)-Ho(1) ^{1}	2.405(3)
N(3)-Ho(2)	2.562(4)	O(7)-Ho(2) ^{1}	2. 412(3)	Ho(2)^{1}-O(11)	2.284(3)
Ho(2)-O(11) ^{2}	2.284(3)	Ho(1)-O(3) ^{1}	2.720(3)	Ho(1)-O(4)	2.446(3)
Compound 5					
Bond	Å	Bond	Å	Bond	Å

Er(1)-O(4)	2.344(4)	Er(2)-O(9^{2})	2.341(4)	Er(3)-N(8)	2.485(6)
Er(1)-O(5)	2.386(4)	Er(2)-O(B^{2})	2.318(4)	Er(3)-O(9)	2.389(4)
Er(1)-O(8)	2.361(4)	Er(2)-O(I)	2.302(4)	Er(3)-O(11)	2.385(4)
Er(1)-O(1)	2.240(4)	Er(2)-O(L)	2.397(5)	Er(3)-N(16)	2.487(5)
Er(1)-O(4)	2.295(4)	Er(3)-O(8)	2.274(5)	Er(02)-O(7)	2.346(4)
Er(1)-O(5)	2.316(4)	Er(2)-N(1)	2.527(6)	O(4)-Er(2)	2.802(4)
Er(1)-N(7)	2.540(5)	Er(2)-N(3)	2.512(6)	O(2)-Er(2)	2.318(4)
Er(1)-N(2)	2.536(5)	Er(3)-O(3)	2.303(4)	O(5)-Er(1)	2.316(4)
Er(2)-O(4^{2})	2.802(4)	Er(3)-O(5)	2.289(4)	O(6)-Er(2)	2.403(4)
Er(2)-O(2)	2.403(4)	Er(3)-O(7)	2.395(5)	O(9)-Er(2)	2.341(4)
Compound 6					
Bond	Å	Bond	Å	Bond	Å
Yb(1)-O(1)	2.375(3)	Yb(2)-O(2W)	2.372(4)	Yb(3)-O(6)	2.279(3)
Yb(1)-O(2)	2.382(4)	Yb(2)-O(3W)	2.320(3)	Yb(3)-O(8)	2.343(3)
Yb(1)-O(3)	2.265(3)	Yb(2)-O(5)	2.300(3)	Yb(3)-O(9)	2.302(3)
Yb(1)-O(7)	2.283(3)	Yb(2)-O(9)	2.841(3)	Yb(3)-O(15)	2.366(3)
Yb(1)-O(13^{1})	2.256(3)	Yb(2)-O(10)	2.363(3)	Yb(3)-O(16^{2})	2.294(3)
Yb(1)-O(1W)	2.353(4)	Yb(2)-O(11)	2.277(3)	Yb(3)-O(17)	2.224(3)
Yb(1)-N(1)	2.464(4)	Yb(2)-N(5)	2.503(5)	Yb(3)-N(3)	2.518(4)
Yb(1)-N(2)	2.473(4)	Yb(2)-N(6)	2.499(5)	Yb(3)-N(4)	2.519(4)
Yb(2)-O(4)	2.327(3)	Yb(2)-C(15)	3.161(5)	O(13)-Yb(1^{1})	2.256(3)

Symmetry transformations used to generate equivalent atoms: For **1**: ^{1}1-X, 1-Y,1-Z; ^{2} +X,+Y,-1+Z; ^{3}1-X,2-Y,-Z. For **2:** ^{1} 1-x, 2-y ,1- z. For **3:** ^{1} 1-x,2-y,1-z; ^{2} –x,1-y,-z . For **4:** ^{1} 'x, y, z ; ^{2} -x, -y, -z' ; For **5**: ^{1} 1-X,1-Y,1-Z; ^{2}+X,+Y,-1+Z;^{3}1-X,2-Y,-Z. For **6**: ^{1} 'x, y, z ; ^{2} -x, -y, -z'

Table S3. Hydrogen bonds parameters for compounds **1-6 [**Å and °**]**

Coordination Polymer 1				
D-H...A	d(D-H)	d(H...A)	d(D...A)	<(DHA)
O(1w)-H(1w)...O(9)	0.84(1)	1.99(2)	2.818(4)	167(4)
O(6)-H(1w)...O(1w)	0.88(1)	1.94(2)	2.803(3)	165(4)
O(3)-H(3w)...O(12)	0.88(1)	1.93(1)	2.799(4)	171(4)
Compound 2				
D-H...A	d(D-H)	d(H...A)	d(D...A)	<(DHA)
O(1w)-H(11)...O(4^{1})	0.838(10)	2.34(4)	2.711(3)	107(3)
O(1w)-H(12)...N(4^{2})	0.836(10)	1.990(15)	2.806(4)	165(4)
N(1)-H(1)...O(6^{3})	0.876(10)	1.945(14)	2.782(3)	159(3)
N(3)-H(3)...O(4^{4})	0.882(10)	1.923(14)	2.783(3)	166(4)
Coordination Polymer 3				
D-H...A	d(D-H)	d(H...A)	d(D...A)	<(DHA)
O(1w)-H(11)...O(2^{1})	0.84	2.30	2.772(4)	112
O(1w)-H(12)...N(4^{1})	0.84	2.06	2.838(5)	152
N(1)-H(1)...O(6^{5})	0.88	2.01	2.812(4)	150
N(5)-H(5)...O(4^{6})	0.88	1.93	2.809(4)	175

Coordination Polymer 4

D-H...A	d(D-H)	d(H...A)	d(D...A)	<(DHA)
O(1w)-H(11)...O(2^{1})	0.84(1)	2.41(4)	2.687(3)	100(3)
O(1w)-H(12)...N(4^{2})	0.84(1)	2.00(1)	2.824(4)	167(4)
N(1)-H(1)...O(6^{3})	0.88(1)	1.95(2)	2.793(3)	161(3)
N(3)-H(3)...O(4^{4})	0.89(1)	1.91(2)	2.783(3)	170(3)

Coordination Polymer 5

D-H...A	d(D-H)	d(H...A)	d(D...A)	<(DHA)
O(1w)-H(11)...O(4^{1})	0.838(10)	2.26(5)	2.688(4)	112(4)
O(1w)-H(12)...N(4^{2})	0.838(10)	1.999(14)	2.833(5)	173(5)
N(2)-H(2)...O(5^{3})	0.881(10)	1.948(16)	2.810(4)	166(4)
N(3)-H(3)...O(2^{4})	0.878(10)	1.927(13)	2.803(4)	174(5)

Coordination Polymer 6

D-H...A	d(D-H)	d(H...A)	d(D...A)	<(DHA)
O(1w)-H(11)...O(4^{1})	0.837(10)	2.32(4)	2.682(4)	107(3)
O(1w)-H(12)...N(4^{2})	0.841(10)	2.012(15)	2.842(5)	169(4)
N(2)-H(2)...O(5^{3})	0.882(10)	1.959(16)	2.821(4)	165(4)
N(3)-H(3)...O(2^{4})	0.881(10)	1.928(14)	2.803(4)	172(6)

Symmetry codes: for **2:** ^{1}-x+1,-y+1,-z+1; ^{2}-x+1,y-1/2,-z+1/2; ^{3}-x+1,y+1/2,-z+1/2; ^{4}x+1,-y+3/2,z+1/2; ^{5}x,-y+3/2,z+1/2; ^{6}x-1,y,z; for **1**, **3**, **4**, **5**: ^{1}1-x, 1-y, 1-z; ^{2}-1+x, 3/2-y, -1/2+z; ^{3}+x, 3/2-y, -1/2+z; ^{4}1+x, +y, +z

References

[1] K. Nakamoto, *Infrared and Raman Spectra of Inorganic and Coordination Compounds*, 4rd, ed. Interscience-Wiley, New York, 1986.

[2] F. N. Shi, L. Cunha-Silva, T. Trindade, F. A. Almeida Paz, and J. Rocha, Crystal Growth & Design, 2009, 9, 2 098–2109.

[3] X. Feng, X.L. Ling, L. Liu, H.L. Song, L.Y. Wang, S.W. Ng, B. Y. Su, A series of 3D lanthanide frameworks constructed from aromatic multicarboxylate ligand: Structural diversity, luminescence and magnetic properties, Dalton Trans. 2013,42 ,10292-10300.